

Global Nonlinear Aerodynamic Model Identification with Multivariate Splines

C.C. de Visser,^{*} J.A. Mulder,[†]

Q.P. Chu[‡]

Delft University of Technology, Delft, The Netherlands

A new method for global nonlinear aerodynamic model identification is presented. This new identification method uses multivariate splines inside a linear regression framework. The linear regression framework allows the use of standard parameter estimation techniques for estimating the parameters of the multivariate splines. The new identification method is used to identify a global nonlinear aerodynamic model of the F-16 fighter aircraft based on simulated flight test data from a NASA subsonic wind tunnel model of the F-16. The high approximation power of the multivariate splines allows the pilot to fly high amplitude, long duration maneuvers resulting in a globally valid, high quality aerodynamic model. The identified aerodynamic model is compared directly with the NASA wind tunnel model showing that the multivariate splines can accurately model both small scale and large scale nonlinear aerodynamic phenomena.

Nomenclature

α	angle of attack
\bar{c}	mean aerodynamic chord
β	angle of sideslip
δ_e	elevator deflection
δ_{lef}	leading edge flap deflection
κ	multi-index
\mathbf{B}	global data location matrix
\mathbf{c}	global B-coefficient vector
\mathbf{D}	global data sifting matrix
\mathbf{H}	smoothness matrix
b	barycentric coordinate
C_m	pitching moment coefficient
C_X	longitudinal force coefficient
C_Z	vertical force coefficient
d	polynomial degree
q	dimensional pitch rate
V	velocity

^{*}Ph.D. student, Control and Simulation Division, Faculty of Aerospace Engineering, P.O. Box 5058, 2600GB Delft, The Netherlands; c.c.devisser@tudelft.nl. Student member AIAA.

[†]Professor, Control and Simulation Division, Faculty of Aerospace Engineering, P.O. Box 5058, 2600GB Delft, The Netherlands; j.a.mulder@tudelft.nl. Member AIAA.

[‡]Associate Professor, Control and Simulation Division, Faculty of Aerospace Engineering, P.O. Box 5058, 2600GB Delft, The Netherlands; Q.P.Chu@tudelft.nl. Member AIAA.

I. Introduction

The identification of high quality global aerodynamic models for aircraft, based on flight data, is a difficult problem. Aircraft dynamics are highly nonlinear and coupled, which means that the effects of individual input dimensions like angle of attack and Mach number on the aerodynamic force and moment coefficients are difficult to separate. The current consensus in aerodynamic model identification is to assume a polynomial model structure for a force or moment coefficient, after which parameter estimation techniques are employed to estimate the parameters of the polynomials such that they, in some way, optimally fit a set of wind tunnel or flight test data.¹⁻⁴ It is well known that polynomials have a limited approximation power which is proportional with the polynomial order. The limited approximation power of polynomials requires the design of flight test maneuvers specifically designed to reduce the effects of dimensional couplings and high order nonlinearities such that the resulting datasets can be adequately modeled with polynomials. In general, these maneuvers are of short duration (e.g. < 10 s) and of low amplitude⁴ which not only limits the volume of data that can be collected, but also limits the coverage of the flight envelope as well as neglecting various nonlinear aerodynamic phenomena.

From the perspective of aerodynamic model identification it would be more desirable to execute long duration, high amplitude maneuvers designed to cover as much of the flight envelope as possible. Polynomial models, however, are inadequate for fitting the datasets resulting from such maneuvers. Many authors have therefore suggested the use of polynomial spline functions for fitting the flight data.⁴⁻⁷ Spline functions are piecewise defined polynomials with a predefined continuity order between pieces. The approximation power of spline functions not only is proportional with the degree of the polynomial but also with the number and density of the polynomial pieces. In the past, multivariate tensor product splines have been used to model aircraft aerodynamics. Smith,⁵ Klein^{6,8} and Bruce⁷ used bivariate tensor product splines in a linear regression framework. It is well known, however, that the multivariate tensor product spline is incapable of fitting scattered data,^{9,10} making it inadequate for the fitting of flight test data, which is inherently scattered.

The objective of this paper is to demonstrate a new identification method based on multivariate simplex splines inside a linear regression framework. The multivariate simplex splines are a new spline type¹¹ which can fit scattered data¹² and have an arbitrarily high approximation power. The linear regression framework for multivariate simplex splines allows the use of standard parameter estimation techniques such as Least Squares (LS) or Maximum Likelihood (ML) for estimating the parameters of the simplex spline polynomials.¹³

The new identification method from¹³ was used to identify a global aerodynamic model for the F-16 fighter aircraft based on simulated flight data. The simulated flight data was generated with a subsonic F-16 flight simulation based on a NASA wind tunnel dataset.¹⁴ A number of long duration, high amplitude maneuvers were flown during which aerodynamic data was collected. With the data, a multivariate simplex spline based aerodynamic model was identified. For reasons of comparison, ordinary polynomial models were also identified using the same dataset. The multivariate spline based, and polynomial models were validated with a subset of the simulated flight data. Results showed that the multivariate spline based aerodynamic model produced a significantly closer fit with the data than the polynomial model. The multivariate spline based, and polynomial models were also compared directly with the F-16 aerodynamic model to test the global behavior of the identified models. These global comparisons showed that the multivariate splines possess the capability to model both small scale and large scale aerodynamic nonlinearities with great accuracy. The polynomial models, on the other hand, can only provide a very rough approximation of global aerodynamic features.

II. Preliminary on Multivariate Simplex Splines

In this section a brief introduction into the mathematical theory of the multivariate simplex spline is given. We would like to refer to¹¹ for an excellent in-depth coverage of the matter.

A. The Simplex and Barycentric Coordinates

The individual spline pieces of the simplex spline are defined on simplices, which are geometric structures that provide a minimal, non-degenerate span of n -dimensional space. For example, the simplex of 2-dimensional space is the triangle and the simplex of 3-dimensional space the tetrahedron. A simplex is defined as follows.

Let V be a set of $n + 1$ unique, non-degenerate, points in n -dimensional space:

$$V = \{v_0, v_1, \dots, v_n\} \in \mathbb{R}^n \quad (1)$$

Then the convex hull of V is the n -simplex t :

$$t = \langle V \rangle \quad (2)$$

The boundary edges of a simplex are called *facets*. A facet of an n -simplex is a $(n - 1)$ -simplex by definition; it is constructed from all but one of the vertices of the n -simplex. Simplices can be joined together so that their facets meet; in that case the set of joined simplices is called a *triangulation*.

The simplex has its own local coordinate system in the form of the barycentric coordinate system. The barycentric coordinate system is instrumental in the definition of the stable local polynomial basis for the multivariate simplex spline. The principle of barycentric coordinates is the following; every point $x = (x_1, x_2, \dots, x_n)$ inside or outside the convex hull of a simplex t , with t as in Eq. (2), can be described in terms of a unique weighted vector sum of the vertices of t . The barycentric coordinate $b(x) = (b_0, b_1, \dots, b_n)$ of x with respect to simplex t are these vertex weights:

$$x = \sum_{i=0}^n b_i v_i \quad (3)$$

The barycentric coordinates are normalized, i.e.

$$\sum_{i=0}^n b_i = 1 \quad (4)$$

B. The B-form of the multivariate simplex spline

The polynomials of the simplex splines can be expressed in the well known B-form,¹⁵ which follows from the multinomial theorem:

$$(b_0 + b_1 + \dots + b_n)^d = \sum_{\kappa_0 + \kappa_1 + \dots + \kappa_n = d} \frac{d!}{\kappa_0! \kappa_1! \dots \kappa_n!} \prod_{i=0}^n b_i^{\kappa_i} \quad (5)$$

At this point the multi-index κ is introduced:

$$\kappa = (\kappa_0, \kappa_1, \dots, \kappa_n) \in \mathbb{N}^{n+1} \quad (6)$$

The 1-norm of the multi-index is given by:

$$|\kappa| = \kappa_0 + \kappa_1 + \dots + \kappa_n = d, \quad d \geq 0 \quad (7)$$

The multi-index provides a convenient mechanism for listing all possible integer permutations that sum up to a value given value, in this case d . The total number of valid permutations of κ is \hat{d} , given by:

$$\hat{d} = \frac{(d + n)!}{n! d!} \quad (8)$$

Using the multi-index from Eq. (6) the multinomial equation Eq. (5) can be simplified into:

$$(b_0 + b_1 + \dots + b_n)^d = \sum_{|\kappa|=d} \frac{d!}{\kappa!} b^\kappa \quad (9)$$

where the factorial of the multi-index $\kappa!$ is equal to the product of factorials as in Eq. (5). The *basis function* $B_\kappa^d(b)$ of the multivariate spline can now be defined as follows:

$$B_\kappa^d(b) := \frac{d!}{\kappa!} b^\kappa \quad (10)$$

In the past, it was proved that $\{B_\kappa^d(b), \kappa \in \mathbb{N}^{n+1}, |\kappa| = d\}$ is a stable basis for the space of polynomials of degree d .^{11,15} This means that any polynomial $p(b)$ of degree d can be written as a linear combination of B_κ^d 's as follows:

$$p(b) = \sum_{|\kappa|=d} c_\kappa B_\kappa^d(b) \quad (11)$$

with c_κ a vector of linear coefficients called control coefficients, or more commonly, *B-coefficients*. The right hand side of Eq. (11) is the so-called *B-form* of the polynomial $p(b)$. The subscript multi-index κ is alternatively called the *indexer* of c .

C. The B-coefficient net

The B-coefficients have a unique spatial location within a simplex. This structure is called the B-coefficient net or *B-net* for short. The graphical representation of the B-net is well known in the literature, see e.g.^{16,17,11} In Fig. 1 the graphical representation of the B-net corresponding with a third degree basis function (i.e. $d = 3$) defined on a triangulation consisting of the three simplices t_i, t_j and t_k is shown. A spline is

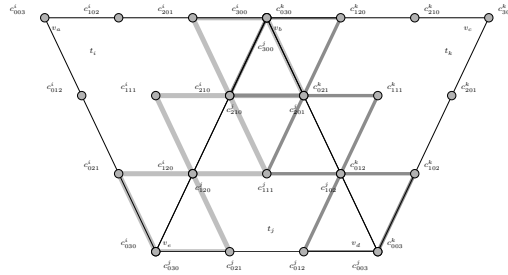


Fig. 1 B-net for third degree basis function on 3 simplices together with C^1 continuity structure

a piecewise continuous function. For simplex splines, the continuity between simplices is described by continuity equations which relate B-coefficients of neighboring simplices. The derivation of the continuity equations is well known, see e.g.^{11–13} In Fig. 1 the graphical interpretation of the C^1 continuity equations for a third order B-net on three simplices is drawn as gray triangles. In total there are 6 continuity equations (i.e. 3 per edge), with which C^1 continuity is achieved across the two simplex edges. Eventually we want all continuity conditions for all facets formulated in the following matrix form:

$$\mathbf{H}\mathbf{c} = 0 \quad (12)$$

Where matrix \mathbf{H} is the so-called smoothness matrix in which every row corresponds to a single continuity equation. The vector \mathbf{c} is the *global* vector of B-coefficients. Vector \mathbf{c} is constructed as follows:

$$\mathbf{c} = [c_\kappa^{t_1} \ c_\kappa^{t_2} \ \dots \ c_\kappa^{t_J}]^T \quad (13)$$

It was proved in¹³ that the smoothness matrix \mathbf{H} is required to be of full rank when it is to be used in a linear regression scheme. Lai shows¹¹ that linear dependencies between continuity equations arise for certain simplex configurations within a triangulation. Care must therefore be taken not to include redundant equations in the smoothness matrix.

III. Linear Regression with Simplex Splines

In this section a brief introduction on linear regression with simplex splines will be given. The linear regression scheme presented here is was first introduced by de Visser,¹³ to which we would like to refer for a more complete coverage of the theory.

A. Linear Regression with B-form Regressors

The standard linear regression model relating a single observation of the dependent variable $y(i)$ with the independent variable $\xi(i)$ is:

$$y(i) = \sum_{m=1}^M \beta_m x_m(\xi(i)) + \epsilon(i) \quad (14)$$

with β_m unknown parameters, $x_m(\xi(i))$ regressors and with $\epsilon(i)$ a residual term. In¹³ it is shown that polynomials in the B-form can be used as regressors as follows:

$$y(i) = \sum_{j=1}^J \left(\delta_{j,k(i)} \sum_{|\kappa|=d} c_{\kappa}^{t_j} B_{\kappa}^d(b(i)) \right) + \epsilon(i) \quad (15)$$

with c^{t_j} the B-coefficients corresponding with simplex t_j , $b(i)$ the barycentric coordinates of the data point $\xi(i)$ with respect to the simplex t_j as in Eq. (3). The sifting operator $\delta_{j,k(i)}$ enforces a local regressor behavior by limiting the regression domain of B-form regressors to their respective simplices. The sifting operator is defined as follows:

$$\delta_{j,k(i)} = \begin{cases} 1, & \text{if } j = k(i) \\ 0, & \text{if } j \neq k(i) \end{cases} \quad (16)$$

with $k(i)$ an index function that produces the index of the simplex which contains the data point $\xi(i)$ inside its convex hull, i.e.:

$$\xi(i) \in t_{k(i)}, \quad \forall i \quad (17)$$

The linear nature of this regression model allows it to be written in a matrix form that includes all measurements on the dependent variable $y(i)$. This matrix form depends on a vector formulation of the B-form introduced in:¹³

$$\sum_{|\kappa|=d} c_{\kappa}^{t_j} B_{\kappa}^d(b(i)) = \mathbf{B}_{t_j}^d(i) \cdot \mathbf{c}^{t_j} \quad (18)$$

with $\mathbf{B}_{t_j}^d$ be the $1 \times \hat{d}$ vector containing the individual terms of the B-form polynomial and with \mathbf{c}^{t_j} be the per-simplex $\hat{d} \times 1$ vector of B-coefficients. We then have for a single observation:

$$\mathbf{B}^d(i) = [\mathbf{B}_{t_1}^d(i) \quad \mathbf{B}_{t_2}^d(i) \quad \cdots \quad \mathbf{B}_{t_J}^d(i)] \quad (19)$$

The non-local, $N \times J \cdot \hat{d}$ regression matrix \mathbf{B}^d that combines all observations $i = 1, 2, \dots, N$ then is:

$$\begin{aligned} \mathbf{B}^d &= \begin{bmatrix} \mathbf{B}^d(1) & \mathbf{B}^d(2) & \cdots & \mathbf{B}^d(N) \end{bmatrix}^T \\ &= \begin{bmatrix} \mathbf{B}_{t_1}^d(1) & \mathbf{B}_{t_2}^d(1) & \cdots & \mathbf{B}_{t_J}^d(1) \\ \mathbf{B}_{t_1}^d(2) & \mathbf{B}_{t_2}^d(2) & \cdots & \mathbf{B}_{t_J}^d(2) \\ \vdots & \vdots & \ddots & \vdots \\ \mathbf{B}_{t_1}^d(N) & \mathbf{B}_{t_2}^d(N) & \cdots & \mathbf{B}_{t_J}^d(N) \end{bmatrix} \end{aligned} \quad (20)$$

To create a local approximation scheme, the global regression matrix \mathbf{B}^d must be multiplied with the block diagonal data sifting matrix \mathbf{D} as introduced in:¹³

$$\mathbf{X} = \mathbf{B}^d \mathbf{D} \quad (21)$$

with \mathbf{X} the *local* regression matrix for all observations. The $N \times 1$ vector \mathbf{Y} that combines all N data values $y(i)$ is:

$$\mathbf{Y} = [y(1) \quad y(2) \quad \cdots \quad y(N)]^T \quad (22)$$

Equivalently, the $N \times 1$ vector ϵ that combines all N model residuals $\epsilon(i)$ is:

$$\epsilon = [\epsilon(1) \quad \epsilon(2) \quad \cdots \quad \epsilon(N)]^T \quad (23)$$

Using Eq. (22), Eq. (21), Eq. (13) and Eq. (23) we can now state the multivariate spline based regression problem in the standard regression form:

$$\mathbf{Y} = \mathbf{X} \mathbf{c} + \epsilon \quad (24)$$

B. Ordinary Least Squares with Equality Constraints

In¹³ two possible parameter estimation techniques for estimating the parameters (i.e. B-coefficients) of the multivariate simplex splines are introduced. In this paper we use an ordinary least squares (OLS) estimator, that is, we assume that the residual vector ϵ is Gaussian white noise. The OLS estimator is subject to a system of equality constraints in the form of the smoothness matrix (i.e. Eq. (12)) which governs the continuity between simplices. The complete, constrained OLS cost function is therefore:

$$J_{OLS}(\mathbf{c}) = \frac{1}{2}(\mathbf{Y} - \mathbf{X}\mathbf{c})^T(\mathbf{Y} - \mathbf{X}\mathbf{c}) \quad \text{subject to} \quad \mathbf{H}\mathbf{c} = 0 \quad (25)$$

with \mathbf{Y} , \mathbf{X} , and \mathbf{c} as in Eq. (24) and \mathbf{H} as in Eq. (12). We use the Lagrange multiplier method as introduced by Awanou¹² to incorporate the equality constraints into the OLS parameter estimator. The final form of the equality constrained OLS parameter estimator is then:

$$\begin{bmatrix} \hat{\mathbf{c}} \\ \hat{\lambda} \end{bmatrix} = \begin{bmatrix} \mathbf{X}^T\mathbf{X} & \mathbf{H}^T \\ \mathbf{H} & 0 \end{bmatrix}^+ \cdot \begin{bmatrix} \mathbf{X}^T\mathbf{Y} \\ 0 \end{bmatrix} \quad (26)$$

with $\hat{\mathbf{c}}$ and $\hat{\lambda}$ estimators for \mathbf{c} and λ respectively. In general, we are only interested in the estimator $\hat{\mathbf{c}}$ and not so much in the vector of Lagrange multipliers $\hat{\lambda}$. Rao shows in¹⁸ that the Moore-Penrose pseudo inverse in Eq. (26) can be factorized as follows:

$$\begin{bmatrix} \mathbf{X}^T\mathbf{\Sigma}^{-1}\mathbf{X} & \mathbf{H}^T \\ \mathbf{H} & 0 \end{bmatrix}^+ = \begin{bmatrix} \mathbf{C}_1 & \mathbf{C}_2 \\ \mathbf{C}_3 & \mathbf{C}_4 \end{bmatrix} \quad (27)$$

with the sizes of the submatrices \mathbf{C}_1 , \mathbf{C}_2 and \mathbf{C}_3 in Eq. (27) equal to the sizes of $\mathbf{X}^T\mathbf{X}$, \mathbf{H}^T and \mathbf{H} respectively. With Eq. (27) and Eq. (26) the final equality constrained OLS estimator for \mathbf{c} is:

$$\hat{\mathbf{c}} = \mathbf{C}_1\mathbf{X}^T\mathbf{Y} \quad (28)$$

IV. Aerodynamic Model Identification of the F-16

In this section an aerodynamic model of the F-16 fighter aircraft is identified using simulated flight test data generated with a non-linear F-16 simulator based on a NASA wind tunnel dataset. The flight test data was obtained by manually flying a number of high amplitude, long duration flight test maneuvers designed to optimally cover the subsonic flight envelope. The identified aerodynamic model is validated by using a set of validation data and by comparing the created aerodynamic models with the known NASA wind tunnel model. We show that the aerodynamic models based on multivariate splines perform significantly better than standard polynomial aerodynamic models, especially if the modeled aerodynamic force or moment coefficient shows highly nonlinear behavior.

A. Flight test maneuver design

The simulated flight test maneuvers were designed to cover the subsonic flight envelope of the F-16 as much as possible, see Fig. 2. In total, 16 long duration (i.e. 60 s), high amplitude maneuvers were flown, resulting in an identification dataset consisting of 60000 data points, and a validation dataset consisting of 12000 data points. The maneuvers were flown manually and consisted of high frequency semi-random aileron, elevator and rudder inputs. The thrust level was kept constant throughout all maneuvers.

B. Aerodynamic model identification

Before starting the process of aerodynamic model identification, the simulated flight data was split into two parts: an identification dataset and a validation dataset. The identification dataset was then used to estimate the parameters of two aerodynamic models: one model based on polynomials, and one on multivariate splines. The parameters of the polynomial model were estimated using a standard least squares estimator such as that used by Klein and Morelli.⁴ For the polynomial model the following model structure was assumed for the longitudinal force and moment coefficients C_X , C_Z and C_m :

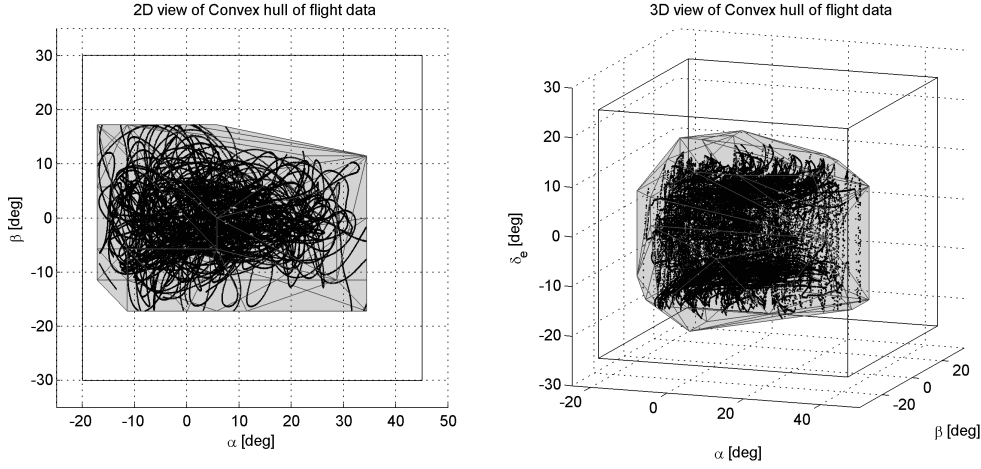


Fig. 2 ADM flight envelope (wire frame cube) and convex hull of flight data (colored volume) together with the data from 16 long duration, high amplitude maneuvers.

$$\begin{aligned}
 F_p(\alpha, \beta, \delta_e, \delta_{lef}, q) = & C_0 + C_\alpha \alpha + C_{\alpha^2} \alpha^2 + C_{\alpha^3} \alpha^3 + C_{\alpha^4} \alpha^4 + C_{\alpha^5} \alpha^5 + \\
 & + C_\beta \beta + C_{\beta^2} \beta^2 + C_{\beta^3} \beta^3 + C_{\beta^4} \beta^4 + C_{\beta^5} \beta^5 + \\
 & + C_q \frac{q\bar{c}}{V} + C_{\alpha q} \alpha \cdot \frac{q\bar{c}}{V} + C_{\delta_e} \delta_e + C_{\delta_{lef}} \delta_{lef}
 \end{aligned} \quad (29)$$

For a single observation of the dependent variable, i.e. the aerodynamic force or moment coefficient we then have:

$$\begin{aligned}
 y(i) = & 1 + C_\alpha \alpha(i) + C_{\alpha^2} \alpha^2(i) + C_{\alpha^3} \alpha^3(i) + C_{\alpha^4} \alpha^4(i) + C_{\alpha^5} \alpha^5(i) + \\
 & + C_\beta \beta(i) + C_{\beta^2} \beta^2(i) + C_{\beta^3} \beta^3(i) + C_{\beta^4} \beta^4(i) + C_{\beta^5} \beta^5(i) + \\
 & + C_q \frac{q(i)\bar{c}}{V} + C_{\alpha q} \alpha(i) \cdot \frac{q(i)\bar{c}}{V} + C_{\delta_e} \delta_e(i) + C_{\delta_{lef}} \delta_{lef}(i)
 \end{aligned} \quad (30)$$

All observations $i = 1, 2, \dots, N$ were then combined in the observation matrix \mathbf{Y} and the regressor vector \mathbf{X} , resulting in the standard linear regression form Eq. (24). The parameters of the model were estimated using an ordinary least squares estimator as follows:

$$\mathbf{C} = (\mathbf{X}^T \mathbf{X})^{-1} \cdot \mathbf{X}^T \cdot \mathbf{Y} \quad (31)$$

with \mathbf{C} the vector of polynomial parameters. For the multivariate spline model the following model structure was assumed:

$$F_s(\alpha, \beta, \delta_e, \delta_{lef}, \frac{q\bar{c}}{V}) = f_1(\alpha, \beta, \delta_e) + f_2(\alpha, \beta) \cdot \delta_{lef} + f_3(\alpha) \cdot \frac{q\bar{c}}{V} + f_4(\alpha) \cdot \frac{q\bar{c}}{V} \cdot \delta_{lef} \quad (32)$$

with f_1 a trivariate spline function, f_2 a bivariate spline function and with f_3 and f_4 univariate spline functions, see Table 1. The spline model structure can be written in the linear regression form for simplex splines as follows:

$$\mathbf{Y} = \left[\mathbf{B}_1 \mathbf{D}_1 \quad \mathbf{B}_2 \mathbf{D}_2 \cdot \delta_{lef} \quad \mathbf{B}_3 \mathbf{D}_3 \cdot \frac{q\bar{c}}{V} \quad \mathbf{B}_4 \mathbf{D}_4 \cdot \delta_{lef} \cdot \frac{q\bar{c}}{V} \right] \cdot [\mathbf{c}_1 \quad \mathbf{c}_2 \quad \mathbf{c}_3 \quad \mathbf{c}_4]^T \quad (33)$$

with the \mathbf{c}_1 to \mathbf{c}_4 the B-coefficient vectors for the spline functions f_1 to f_4 respectively. The regression problem in Eq. (33) can be solved for the B-coefficient vectors using the equality constrained least squares estimator from Eq. (28). In order to enforce continuity between spline pieces, a global smoothness matrix

Table 1 Spline function properties

function	variables	degree	continuity	simplex count
f_1	α, β, δ_e	5	C^1	450
f_2	α, β	3	C^1	98
f_3	α	5	C^1	12
f_4	α	5	C^1	12

\mathbf{H}_g needs to be defined which combines the continuity conditions of all 4 spline regressors. The global smoothness matrix \mathbf{H}_g in this case is:

$$\mathbf{H}_g = \begin{bmatrix} \mathbf{H}_1 & 0 & 0 & 0 \\ 0 & \mathbf{H}_2 & 0 & 0 \\ 0 & 0 & \mathbf{H}_3 & 0 \\ 0 & 0 & 0 & \mathbf{H}_4 \end{bmatrix} \quad (34)$$

with \mathbf{H}_1 to \mathbf{H}_4 the full rank smoothness matrices for the spline functions f_1 to f_4 respectively. Substitution of Eq. (33) for \mathbf{Xc} and Eq. (34) for \mathbf{H} in Eq. (28) leads to the following estimator for the combined B-coefficient vector:

$$\begin{bmatrix} \mathbf{c}_1 \\ \mathbf{c}_2 \\ \mathbf{c}_3 \\ \mathbf{c}_4 \end{bmatrix} = \mathbf{C}_1 \mathbf{X}^T \mathbf{Y} \quad (35)$$

with \mathbf{C}_1 the upper left block of the (pseudo) inverse of the information matrix as in Eq. (27) and \mathbf{X} and \mathbf{Y} as in Eq. (33).

C. Aerodynamic model validation

The polynomial and multivariate spline based aerodynamic models were validated against the validation dataset. To validate the identified models, the control surface deflections measured during the maneuvers was used as input in the identified models. The difference between the true and the predicted aerodynamic coefficients was then calculated for both model types.

The results from the model validation for the pitching moment coefficient C_m is shown in figure Fig. 3. In Fig. 4 a detailed view of the validation maneuver is shown. The figure clearly shows that the output from the multivariate spline based aerodynamic model better matches the true output from the NASA wind tunnel model than the polynomial model; The spline model has a relative error RMS of 0.35% while the polynomial model has a 2.30% relative error RMS (also see Table 2).

In Fig. 5 the results from the aerodynamic model validation for the longitudinal force coefficient C_X is shown. In Fig. 5 a detail view of the model validation is shown. The difference between the performance of the spline model and the polynomial model is more pronounced for the longitudinal force coefficient; the spline model obtains a 0.34% relative error RMS, while the polynomial model has a relative error RMS of 4.77% (also see Table 2).

The results from the aerodynamic model validation for the longitudinal force coefficient C_Z is shown in Fig. 7, while Fig. 7 shows a detail view of the validation. These figures clearly show that the performance of the multivariate spline based model and the polynomial model are much closer. In fact, the spline model has a relative error RMS of 0.50% while the polynomial model scores a relative error RMS of 0.89%. As we will show in the next section, this is explained by the fact that the C_Z force coefficient is a much less complex function than the C_m and C_X coefficients. In this case, a polynomial model provides adequate approximation performance, while the use of multivariate splines could be considered overkill.

D. Model comparison

Because the true aerodynamic model of the F-16 simulator is known in the form of the NASA wind tunnel data tables, we can perform a direct comparison between the true and the identified aerodynamic models.

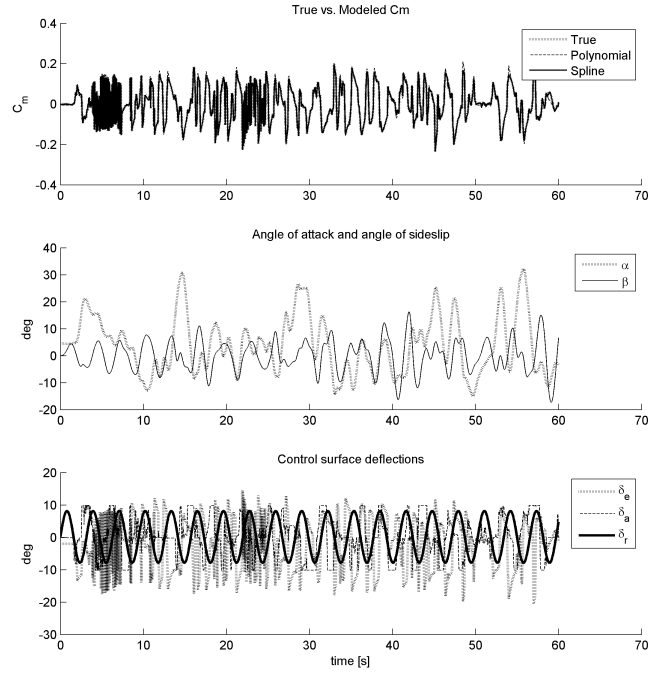


Fig. 3 Input and output variables of the estimated aerodynamic models for C_m , together with the true value of C_m

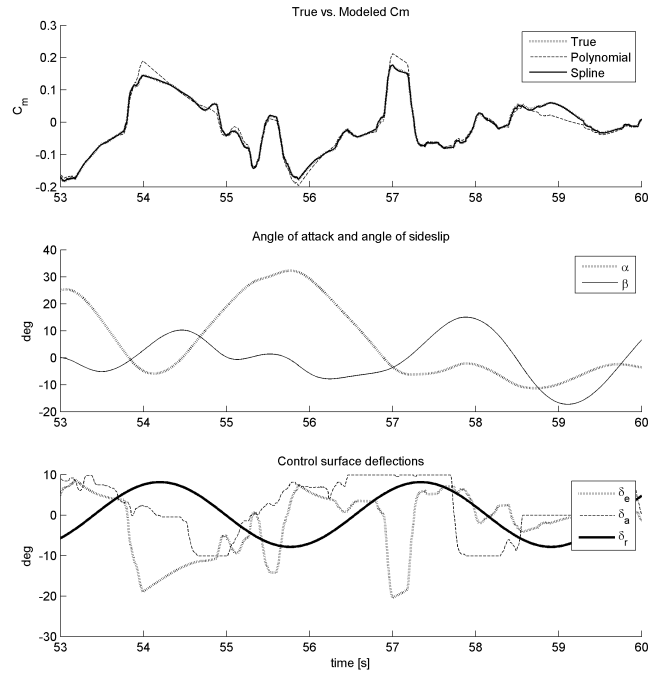


Fig. 4 Detail view of the input and output variables of the estimated aerodynamic models for C_m , together with the true value of C_m

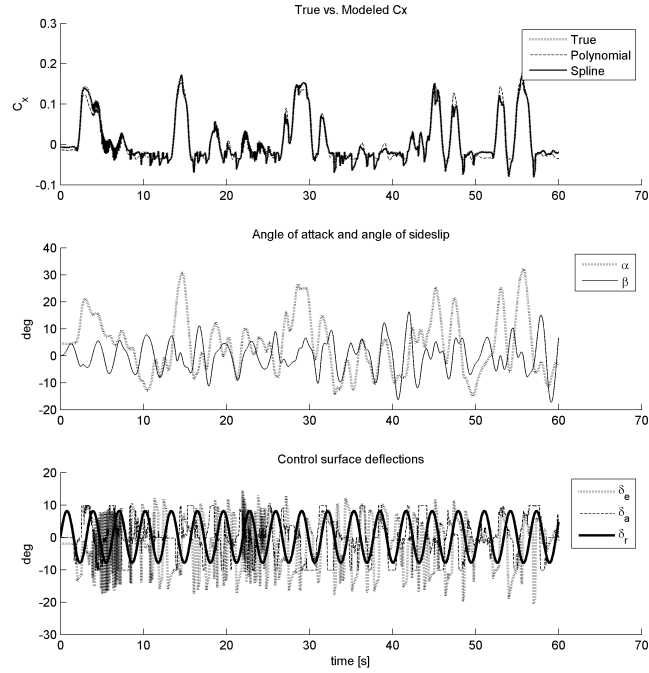


Fig. 5 Input and output variables of the estimated aerodynamic models for C_X , together with the true value of C_X

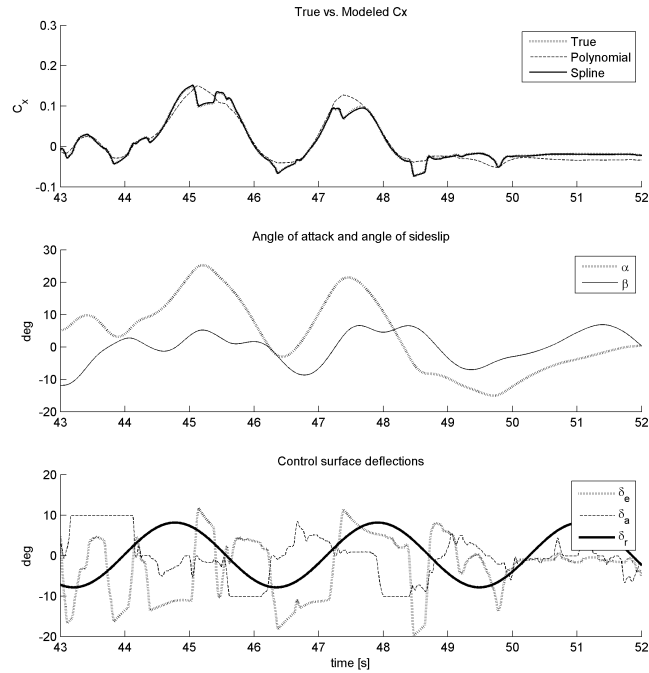


Fig. 6 Detail view of the input and output variables of the estimated aerodynamic models for C_X , together with the true value of C_X

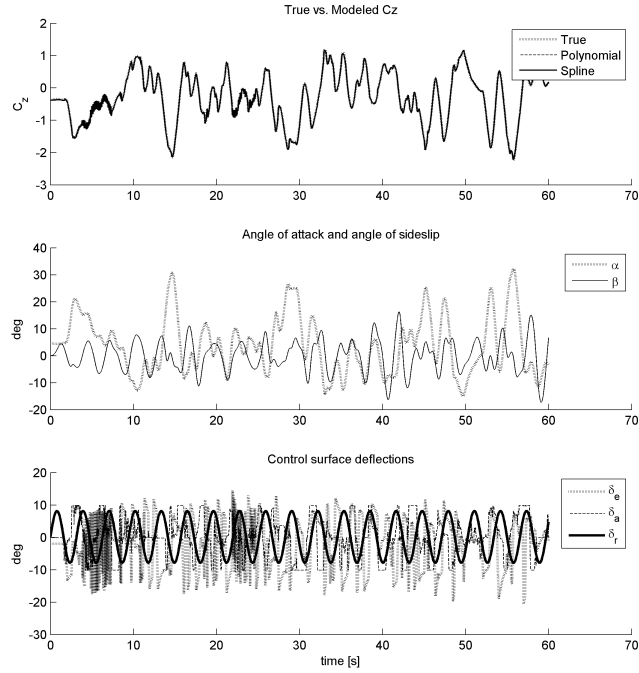


Fig. 7 Input and output variables of the estimated aerodynamic models for C_Z , together with the true value of C_Z

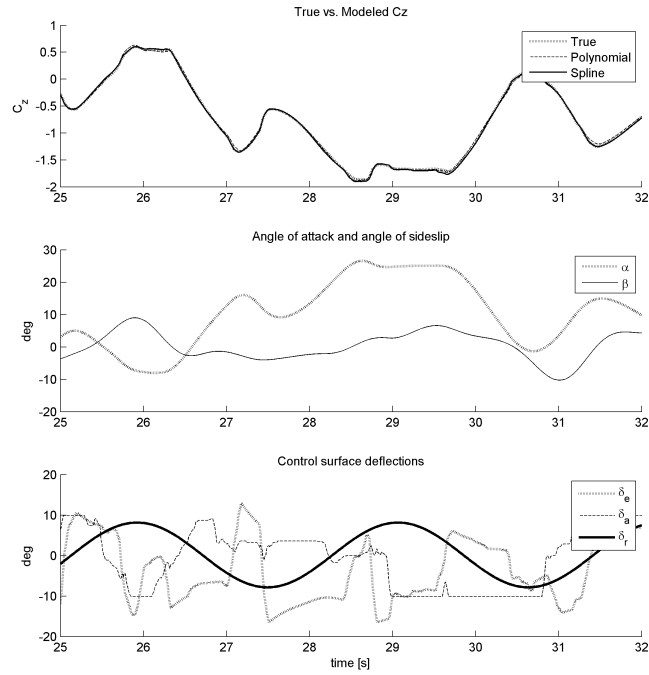


Fig. 8 Detail view of the input and output variables of the estimated aerodynamic models for C_Z , together with the true value of C_Z

For this, a surface grid is defined over which the true and identified aerodynamic models are evaluated. In Fig. 9 surface plots of the aerodynamic pitching moment coefficient C_m is shown. These surfaces were generated using $\delta_{lef} = 0^\circ$ and $\frac{q\bar{c}}{V} = 0$. This figure clearly shows the nonlinearity of the pitching moment coefficient, as well as the ability of the multivariate splines to accurately model these nonlinearities. The polynomial model, on the other hand, only produces a very rough approximation of the general shape of the C_m function. In Fig. 9 line plots of C_m are drawn as a function of the angle of attack for three different side slip angles. This figure again shows the close correspondence between the true C_m and the multivariate spline based model.

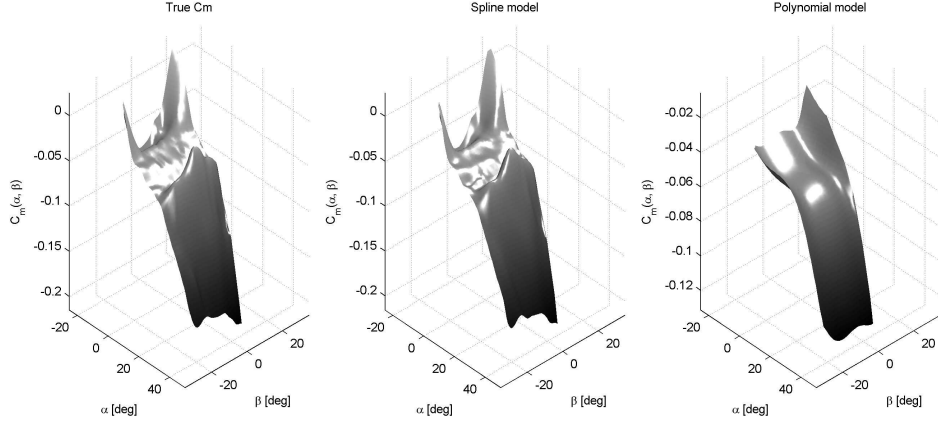


Fig. 9 $C_m(\alpha, \beta)$ surface plots of true (left), spline (middle), and polynomial models (right)

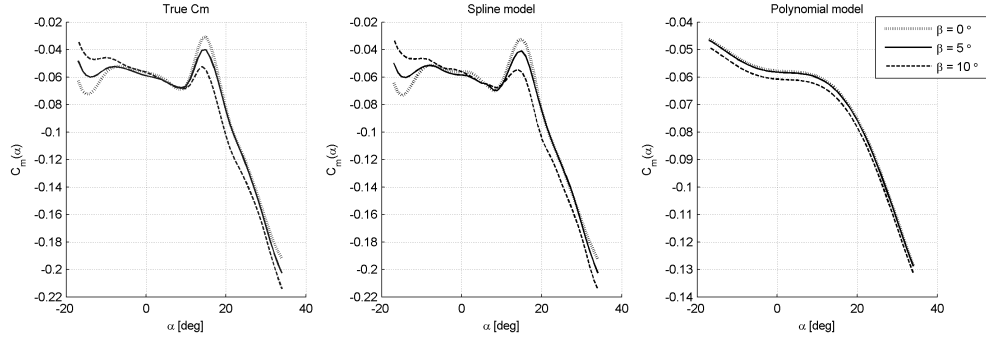


Fig. 10 $C_m(\alpha)$ line plots of true (left), spline (middle), and polynomial models (right)

In Fig. 11 the surface plots for the longitudinal force coefficient C_X are shown. The wind tunnel model of C_X clearly is very nonlinear. From the figure it is clear that the multivariate splines provide the necessary approximation power to model C_X . The polynomial model is clearly incapable of adequately modeling this force coefficient. The line plots in Fig. 12 confirm this observation.

The vertical force coefficient C_Z shows a completely different picture, as can be seen in Fig. 13. This particular aerodynamic coefficient has a relatively linear behavior. As a result, the polynomial model is able to adequately model this coefficient to almost the same accuracy as the multivariate spline model. These results explain why the validation results of the spline model and the polynomial models were so close (i.e. 0.50% vs 0.89%).

V. Conclusion

In this paper, we present a new method for aerodynamic model identification based on multivariate simplex splines. We show that standard parameter estimation techniques, like ordinary least squares, can be used to estimate the parameters of the multivariate simplex splines. The new identification method

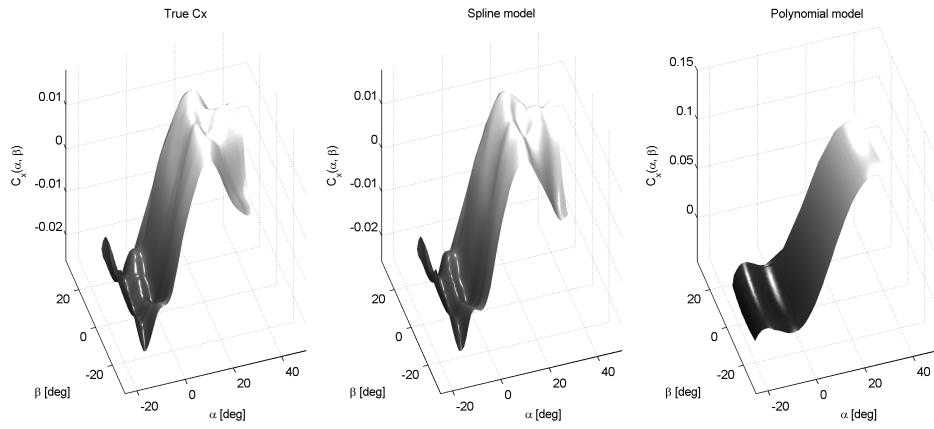


Fig. 11 $C_X(\alpha, \beta)$ surface plots of true (left), spline (middle), and polynomial models (right)

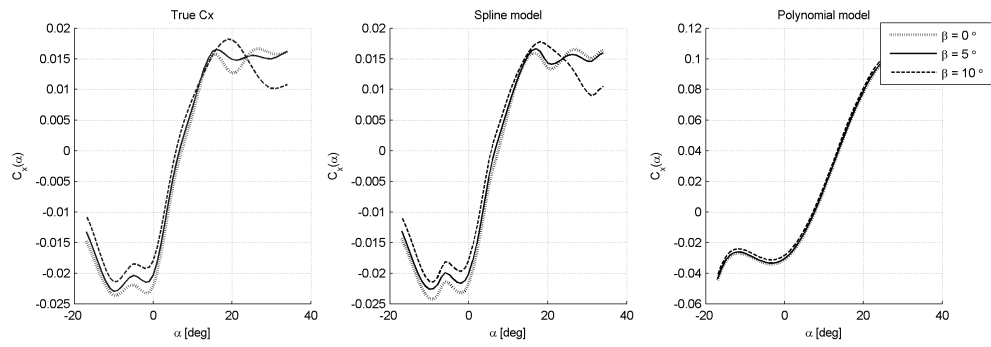


Fig. 12 $C_X(\alpha)$ line plots of true (left), spline (middle), and polynomial models (right)

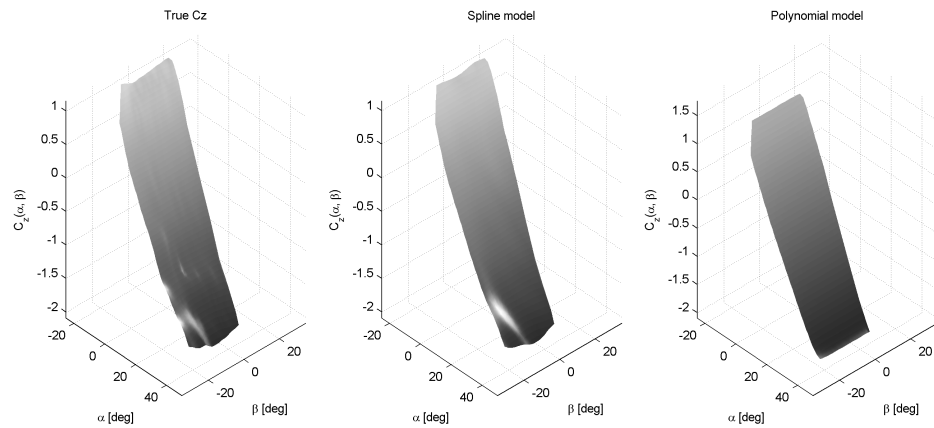


Fig. 13 $C_Z(\alpha, \beta)$ surface plots of true (left), spline (middle), and polynomial models (right)

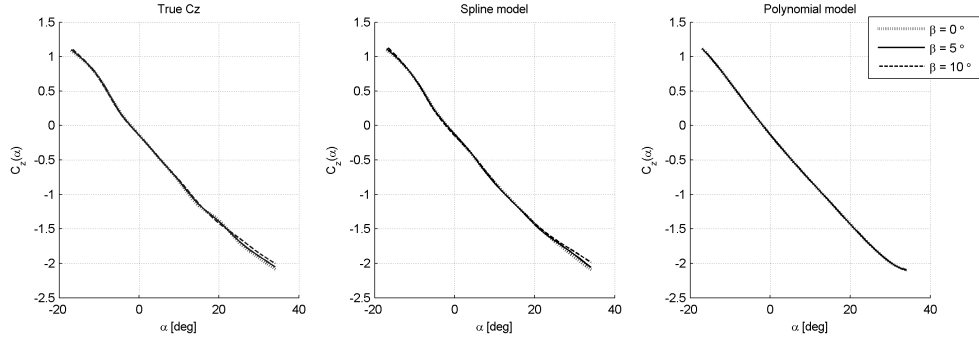


Fig. 14 $C_Z(\alpha)$ line plots of true (left), spline (middle), and polynomial models (right)

Table 2 Model performance parameters

Performance parameter	Spline model (error RMS)	Polynomial model (error RMS)
C_m validation	0.35%	2.30%
C_m ADM comparison	0.54%	11.53%
C_X validation	0.34%	4.77%
C_X ADM comparison	1.13%	113.80%
C_Z validation	0.50%	0.89%
C_Z ADM comparison	0.58%	2.03%

was demonstrated on a set of flight data created with a nonlinear F-16 simulator. In order to compare the performance of the new identification method with current standard methods, ordinary polynomial models were also created based on the same flight data. Because the exact aerodynamic model of the F-16 simulator is known, a direct comparison between the true model, the multivariate spline based model, and the polynomial model could be made. These comparisons showed that multivariate simplex splines have the ability to model small scale as well as large scale nonlinear aerodynamic effects with great accuracy, providing near perfect aerodynamic models. Standard polynomial models, on the other hand, can only provide a rough approximation of the global aerodynamic behavior while completely missing small scale details. For the model of the pitching moment coefficient C_m , for example, the multivariate spline model has a relative global error RMS of 0.54%, while the polynomial model for C_m has a relative global error RMS of 11.53%.

We conclude that multivariate simplex splines, used inside a linear regression framework, provide an extremely significant increase in modeling accuracy compared with standard polynomials. Multivariate splines can globally approximate both small and large scale system nonlinearities with unprecedented accuracy, while polynomials can only provide rough approximations of global system features. Because of this capability, the new identification method presented in this paper is a potentially highly desirable tool in the design of control systems for nonlinear systems like high performance aircraft.

References

- ¹Morelli, E. A. and Klein, V., "Accuracy of Aerodynamic Model Parameters Estimated From Flight Test Data," *AIAA Journal of Guidance Control and Dynamics*, Vol. 20, 1997, pp. /.
- ²Morelli, E. A., "Global Nonlinear Parameteric Modeling with Application to F-16 Aerodynamics," *American Control Conference*, 1998.
- ³Waelkens, S., Chu, Q., and J.A. Mulder, J. A., "Aerodynamic Model Identification from Flight Data for the Eclipse 500 Very Light Jet," *AIAA Guidance, Navigation and Control Conference and Exhibit*, 2005.
- ⁴Klein, V. and Morelli, E. A., *Aircraft System Identification*, AIAA, 2006.
- ⁵Smith, P. L., "Curve Fitting and Modeling with Splines Using Statistical Variable Selection Techniques," Contractor Report NASA-CR-166034, NASA, 1982.
- ⁶Klein, V. and Batterson, J. G., "Determination of Airplane Model Structure From Flight Data Using Splines and Stepwise Regression," Tech. Rep. 2126, NASA, 1983.

- ⁷Bruce, P. D. and Kellett, M. G., "Modelling and identification of non-linear aerodynamic functions using B-splines," *Proceedings of the Institution of Mechanical Engineers, Part G: Journal of Aerospace Engineering*, Vol. 214, 2000, pp. 27–40.
- ⁸Klein, V., "Estimation of Aircraft Aerodynamic Parameters from Flight Data," *Progress in Aerospace Sciences*, Vol. 26, 1989, pp. 1–77.
- ⁹Clenshaw, C. W. and Hayes, J. G., "Curve and Surface Fitting," *Journal of Applied Mathematics*, Vol. 1, 1965, pp. 164–183.
- ¹⁰Anderson, I. J., Cox, M. G., and Mason, J. C., "Tensor-Product Spline Interpolation to Data On or Near a Family of Lines," *Numerical Algorithms*, Vol. 5, 1993, pp. 193–204.
- ¹¹Lai, M. J. and Schumaker, L. L., *Spline Functions over Triangulations*, Cambridge University Press, 2007.
- ¹²Awanou, G., Lai, M. J., and Wenston, P., "The Multivariate Spline Method for Scattered Data Fitting and Numerical Solutions of Partial Differential Equations," *Wavelets and Splines*, 2005.
- ¹³de Visser, C. C., Chu, Q. P., and Mulder, J. A., "A New Approach to Linear Regression with Multivariate Splines," *Automatica*, 2009, accepted for publication.
- ¹⁴Nguyen, L. T., Ogburn, M. E., Gilbert, W. P., Kibler, K. S., Brown, P. W., and Deal, P. L., "Simulator Study of Stall/Post-Stall Characteristics of a Fighter Airplane With Relaxed Longitudinal Static Stability," Technical Report 1538, NASA, 1979.
- ¹⁵de Boor, C., "B-form Basics," *Geometric modeling: algorithms and new trends*, edited by G. Farin, SIAM, 1987.
- ¹⁶Farin, G., "Triangular Bernstein-Bézier Patches," *Computer Aided Geometric Design*, Vol. 3, 1986, pp. 83–127.
- ¹⁷Lai, M. J., "Geometric Interpretation of Smoothness Conditions of Triangular Polynomial Patches," *Computer Aided Geometric Design*, Vol. 14, 1997, pp. 191–199.
- ¹⁸Rao, C. R., *Linear Statistical Inference and Its Applications*, John Wiley & Sons, Inc., 2002.